Available online at www.sciencedirect.com
SCIENCE DIRECT®
Earth and Planetary Science Letters 248 (2006) 253–262
EPSL
www.elsevier.com/locate/epsl

Sea ice control of Plio–Pleistocene tropical Pacific climate evolution

Shih-Yu Lee *, Christopher J. Poulsen

Department of Geological Sciences, University of Michigan, 1100 N. University Avenue, Ann Arbor, MI 48109, USA

Received 13 March 2006; received in revised form 24 May 2006; accepted 24 May 2006
Available online 7 July 2006
Editor: M.L. Delaney

Abstract

Marine proxies of sea surface temperature (SST) indicate that the tropical Pacific thermal gradient intensified through the Plio–Pleistocene and peaked during Pleistocene glaciations. The cause of this variability, which has been linked to the initiation of the Walker circulation, is uncertain. Here, we hypothesize that Plio–Pleistocene tropical climate variability was coupled to high-latitude Southern Hemisphere climate change, specifically sea-ice extent. We use a coupled ocean–atmosphere general circulation model to investigate the influences of sea-ice extent and atmospheric CO_2 on the tropical Pacific thermal structure. In the model, CO_2-radiative forcing in the absence of any sea-ice feedbacks has little influence on the tropical SST gradient. A 180 ppm reduction in CO_2 causes the SST gradient to decrease by 0.4 °C. In comparison, an expansion of Southern Hemisphere, high-latitude sea ice reduces tropical SSTs and enhances the SST gradient in the tropical Pacific by as much as 3.5 °C. Tropical cooling is primarily due to the advection and upwelling of waters into the eastern equatorial Pacific that were cooled by sensible heat loss at the sea-ice margin in the Southern Pacific. An energy balance analysis indicates that the ocean heat flux into the eastern equatorial Pacific decreases by ~44%. This mechanism provides an intimate coupling between the tropical Pacific and the high-latitude Southern Hemisphere through the thermocline circulation.

Keywords: sea ice; CO_2; tropical Pacific; sea surface temperature; Plio–Pleistocene; ice age

1. Introduction

The modern tropical Pacific Ocean is characterized by an east–west thermal gradient with a pool of warm water in the western equatorial Pacific (WEP) and a tongue of colder water in the eastern equatorial Pacific (EEP). The sea surface temperature gradient is largely set by the thermocline depth in the EEP; shoaling of the thermocline due to upwelling of subsurface waters offshore of Peru cools the EEP surface waters, intensifying the tropical SST gradient [1]. The thermal structure of the tropical Pacific is tightly coupled with the zonal overturning circulation in the atmosphere, the Walker circulation. As first postulated by Bjerknes [2], an increase of the SST gradient across the Pacific is associated with higher precipitation and sea-surface pressure gradients, stronger easterlies, and an intensification of the Walker circulation. Through this coupling with the Walker circulation, the zonal Pacific SST gradient figures significantly in the global exchange of heat, moisture, and momentum.

It is important to consider then that the modern tropical Pacific SST gradient is a relatively young feature and may have been absent as recently as the

* Corresponding author. Tel.: +1 734 647 5636; fax: +1 734 763 4690.
E-mail address: shihyu@umich.edu (S.-Y. Lee).

0012-821X/$ - see front matter © 2006 Elsevier B.V. All rights reserved.
doi:10.1016/j.epsl.2006.05.030

Pliocene [3,4]. Marine proxy records of tropical Pacific seawater temperature indicate that the east–west SST gradient has likely increased by ~2 °C over the last 1.75 my as the EEP has gradually cooled [5–9]. This secular trend in the east–west SST gradient is only part of the story. Glacial–interglacial fluctuations of equivalent magnitude are superimposed on this long-term trend [6,7]. Assuming that ocean–atmosphere interactions have not fundamentally changed since the Pliocene, increases in the tropical Pacific SST gradient through the Pleistocene and during interglacial–glacial transitions were likely accompanied by intensification of the large-scale Walker circulation [5–8,10].

The cause of the Plio–Pleistocene evolution of the tropical Pacific is uncertain. The tropical thermocline depth is set by the temperature of the mid-latitude waters that source the thermocline and the rate at which these waters are upwelled, a process that is largely controlled by the local wind stress [11]. Two specific mechanisms have been given for the long-term Plio–Pleistocene shoaling of the thermocline: 1) secular cooling of deep waters through the Cenozoic [10], and 2) intensification of the southeast trades resulting from an equatorward shift in the Antarctic Circumpolar Current after 1.83 my [7]. Neither of these mechanisms account for the glacial–interglacial variations in tropical SST gradient.

Glacial–interglacial variations in tropical Pacific SST gradient are not completely unexpected. Paleoclimate data indicate an increase in EEP upwelling during the Last Glacial Maximum (LGM) and earlier Pleistocene glacials [12–16]. Climate model simulations of the LGM support the paleo-data, predicting enhanced upwelling, cooling of EEP SST, and shallowing of the tropical thermocline [17–19]. However, the reduction in the east–west SST gradient was unlikely to be symptomatic of glacial conditions, because Pacific tropical climate change preceded Northern Hemisphere glaciations by several thousand years [20]. The cause of glacial–interglacial tropical Pacific SST gradient changes has not been specifically addressed in the literature. However, Medina-Elizalde and Lea [8] ascribe the general evolution of tropical SSTs between glacial and interglacial periods to direct radiative forcing by atmospheric CO_2.

In this contribution we propose that the evolution of the Pacific SST gradient was largely tied to the expansion and contraction of Southern Ocean sea ice. That the sea-ice margin evolved through the Plio–Pleistocene is well documented, though the details are not highly resolved. It is known that the Pliocene sea-ice margin was substantially retracted relative to the modern [21] and protracted during the LGM [22]. If the LGM and present-day are representative of glacial and interglacial intervals, it is to be expected that the sea-ice margin expanded and contracted in concert with the Pleistocene glacial–interglacial cycles. The sea-ice margin is important because it exerts a strong control on the sensible heat loss, and consequently the temperature, of the mid-latitude seawater that is subducted and advected through the eastern boundary current to form the waters at the base of the thermocline in the EEP [23]. As demonstrated in Lee and Poulsen [23], the expansion of Southern Ocean sea ice and the reduction of mid-latitude SST lead to a cooling of EEP waters. This sea-ice-thermocline mechanism provides a strong link of communication between the Southern Hemisphere high-latitude and tropical climates, explaining the near synchronicity in proxy records from these regions. We hypothesize that this mechanism tied the secular and glacial–interglacial trends in the tropical Pacific climate to the Southern Ocean sea-ice history.

The purpose here is to provide a proof-of-concept of our hypothesis. To this end, we present results from a series of coupled ocean–atmosphere experiments in which the sea-ice extent is imposed; simulations of Pliocene and Pleistocene sea ice will be addressed in a future study. After explaining our methodology (Section 2), we describe the model results (Section 3). In Section 3.1, we explore how the tropical Pacific Ocean responds to imposed high-latitude sea-ice forcing. In Sections 3.2 and 3.3, we describe the tropical SST response to a reduction in atmospheric CO_2 with and without the sea-ice feedback.

In Section 4, we discuss the implications of our model results in light of Plio–Pleistocene marine proxy data and paleoceanographic evidence of sea ice evolution.

2. Method and model description

2.1. FOAM

This study was completed using the Fast Ocean Atmosphere Model (FOAM) version 1.5, a fully coupled mixed-resolution ocean and atmosphere GCM [24]. The atmospheric model is a parallelized version of the Community Climate Model 2 (CCM2) with the upgraded radiative and hydrological physics incorporated in CCM3.6 [25]. The atmospheric component of FOAM was run at a spectral resolution of R15 (4.5° × 7.5°) with 18 vertical levels. The oceanic component (OM3) is a *z*-coordinate ocean model with 128 × 128 point Mercator grid (1.4° × 2.8°), 24 vertical levels, and an explicit free surface. The sea-ice model in

Table 1
Experiments and winter sea-ice extent

Experiment	CO_2 level (ppmv)	Mean winter sea-ice area (10^7 km^2)	
		DJF N.H.	JJA S.H.
MOD-ICE	200	1.76	2.41
LGM-ICE	200	2.09	4.68
LGM-ICE380	380	1.85	3.61
NO-ICE	200	0.00	0.00
NO-ICE380	380	0.00	0.00

See Section 2.2 for a description of our methodology for specifying the sea ice (DJF = December, January, February; JJA = June, July, August; N.H. = Northern Hemisphere; S.H. = Southern Hemisphere).

FOAM uses the thermodynamic component of the CSM1.4 sea-ice model, which is based on the Semtner 3-layer thermodynamic snow/ice model [27]. A coupler component interpolates fluxes between the atmospheric, oceanic, and sea-ice models to accommodate their different time steps and grid settings. FOAM was designed for long century-scale integrations and exhibits minimal ocean drift with no flux corrections [26]. FOAM's simulation of modern climate shows reasonable agreement with present-day observations. FOAM has been widely used to study climate change through geological time (e.g. [28–30]).

2.2. Experimental design

In this study, we use FOAM to estimate the tropical climate response to the extent of sea-ice in the high latitudes. To this end, three experiments were completed with extensive, moderate, and no amounts of sea ice (Table 1). In order to specify different sea-ice extents under otherwise identical boundary conditions, we tuned a model parameter that maps the sea-ice extent from the sea-ice model to the coupler. Under LGM boundary conditions (described below) and no tuning, FOAM predicts about 10% too much sea ice in the Southern Ocean during winter. As a result, in all cases, our tuning reduced the sea-ice amount. It is important to note that by reducing the sea-ice extent, we artificially add latent energy to the high-latitude oceans with more energy added in the more highly tuned cases. This sea-ice tuning is justified by the purpose of this study, to assess the degree to which the sea-ice extent regulates the tropical Pacific climate.

The mean winter sea-ice areas predicted through our tuning procedure are listed in Table 1. The differences in global sea-ice distribution occur mainly in the Southern Hemisphere and North Atlantic with smaller differences in the North Pacific (Table 1 and Fig. 1). The case with the largest sea-ice extent compares well with paleo sea-ice reconstructions for the LGM with the exception that slightly more sea ice is present in the South Pacific and North Pacific Ocean than observed [22,31]. The case with moderate sea-ice extent is similar to the modern sea-ice coverage [32]. Hereafter we will refer to these cases as the LGM-ICE, MOD-ICE, and NO-ICE experiments. In addition to these three experiments, two additional experiments were conducted with elevated atmospheric CO_2 concentrations (Table 1), representing Pliocene levels [34], to evaluate the influence of CO_2 on tropical Pacific climate.

We chose to use boundary conditions for the most recent glacial episode (i.e. the LGM) because it represents a time of maximum sea-ice extent and provides the greatest contrast with the Pliocene when sea-ice extent was most reduced. All FOAM experiments were initialized with LGM boundary conditions that include ice-sheet elevations and extents, sea level, topography, vegetation, orbital settings, and greenhouse

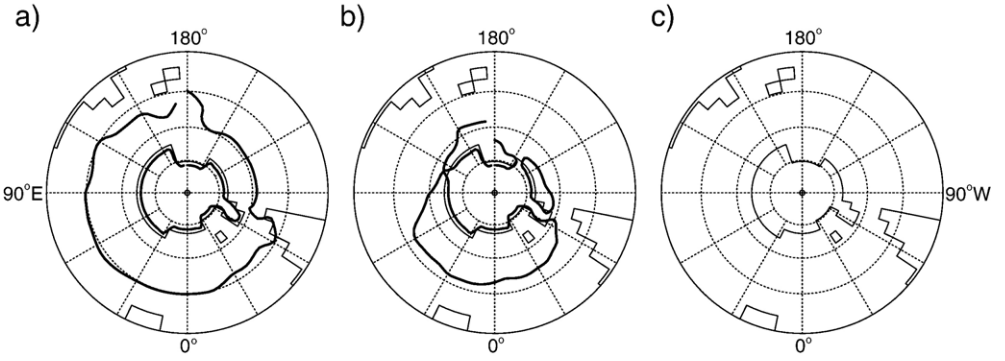

Fig. 1. Mean Southern Hemisphere winter (June–July–August) sea-ice distribution for the LGM-ICE (left), MOD-ICE (middle), and NO-ICE (right) experiments. The LGM-ICE winter sea-ice extent is approximately 95% greater than the MOD-ICE. NO-ICE has no sea ice by design (see Section 2.2). The polar projection map begins at 30°S.

Table 2
Summary of Last Glacial Maximum boundary conditions

Parameter	Reference	Description
Ice sheet extent	Peltier [56]	LGM Antarctic and northern hemisphere continental glacials
Topography	Peltier [56]	LGM condition with glacial topography and reduced sea level
Vegetation	Peltier [56]	LGM condition
CO_2	Petit et al. [45]	200 ppmv
CH_4	Petit et al. [45]	400 ppbv
N_2O	Petit et al. [45]	275 ppbv
Orbital setting	Berger [55]	LGM configuration

gases appropriate for 21,000 ka (Table 2). The model experiments were integrated for 200 yrs, bringing the surface ocean into equilibrium. Model results were averaged over the last 20 yrs of the experiments.

3. Results

3.1. Sea-ice forcing and tropical Pacific climate

The high-latitude sea-ice extent has a substantial influence on both high and low latitude SSTs (Fig. 2). Tropical zonal average SSTs differ by about 5 °C between the LGM-ICE and NO-ICE experiments and 2 °C between the MOD-ICE and NO-ICE experiments. High-latitude sea-ice amounts also influence the tropical Pacific zonal thermal gradient. Larger sea-ice amounts in the Southern Ocean cause a reduction in the average tropical SST and an enhancement of the east–west SST gradient (Fig. 3). For example, in comparison to the NO-ICE case, the tropical east–west SST gradients in the MOD-ICE and LGM-ICE experiments are ~1.0 and ~3.5 °C greater. In both cases, the enhanced SST gradient results from greater cooling in the EEP than the WEP.

The sea-ice extent controls high-latitude SSTs mainly through its influence on sensible heat loss in the mid-

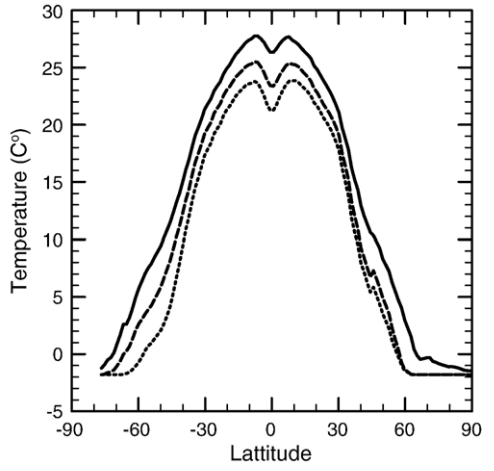

Fig. 2. Simulated mean-annual SST in LGM-ICE (dotted), MOD-ICE (dashed), and NO-ICE (solid) experiments. LGM-ICE and MOD-ICE SSTs are approximately 10 and 6 °C cooler than NO-ICE at 45°S.

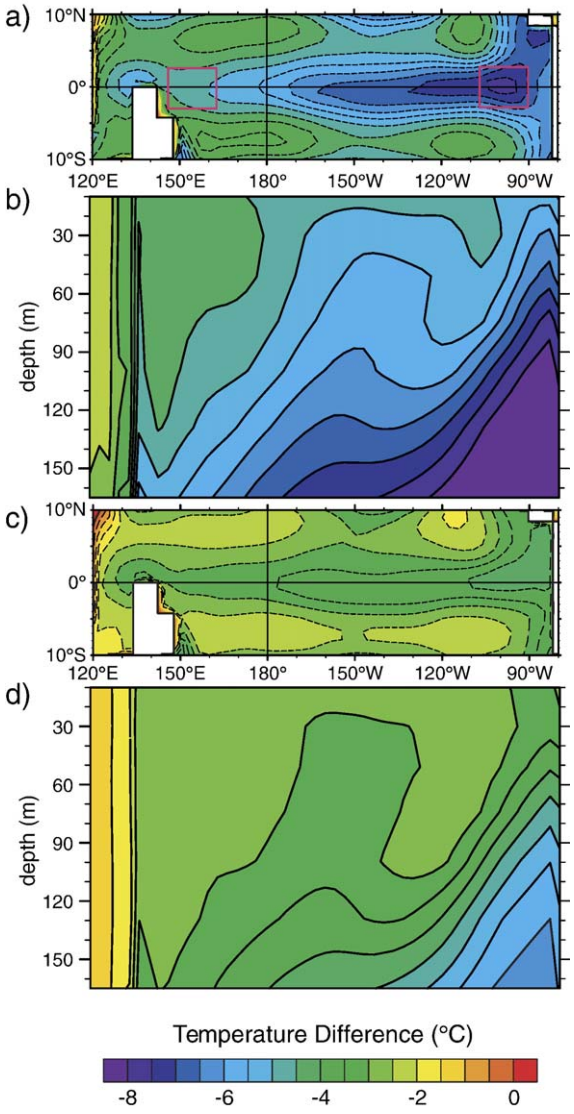

Fig. 3. Mean-annual SST differences (°C) in the equatorial Pacific Ocean between (a) the LGM-ICE and NO-ICE experiments, and (c) the MOD-ICE and NO-ICE experiments. In both cases, the presence of high-latitude sea ice causes tropical cooling with greater cooling in the EEP, intensifying the east–west tropical SST gradient. Cross section of mean-annual seawater temperature difference (°C) between (b) the LGM-ICE and NO-ICE experiments, and (d) the MOD-ICE and NO-ICE experiments. Pacific temperature differences are averaged between 10°N and 10°S. Note that much colder waters are upwelled in the EEP in the experiments with sea ice. The contour interval is 0.5 °C.

latitude regions. As sea ice advances equatorward, the advection of cold air from the sea-ice surface to the sea surface enhances the mean-annual sensible heat loss. In the mid-latitude (40–50°S) Southern Ocean, mean-annual sensible heat losses are 8.4 and 4.9 W m^{-2} greater and up to 28 and 12 W m^{-2} higher along seasonal sea-ice margin in the LGM-ICE and MOD-ICE experiments than in the NO-ICE case. As a result, mid-latitude SSTs are 7 and 3 °C lower (Fig. 2).

The coupling between high-latitude sea-ice area and tropical SSTs occurs through the thermocline circulation. In FOAM, mid-latitude South Pacific seawater, cooled by sensible heat loss, is subducted and advected through the eastern boundary Peru current until it is eventually upwelled in the eastern tropical Pacific. Increasing the sea-ice extent reduces the temperature of the mid-latitude waters that source the EEP. This result is shown in Fig. 3; in comparison to the NO-ICE case, at 90m depth subsurface waters upwelled in the EEP are 8 and 5 °C colder in the LGM-ICE and MOD-ICE experiments. The expansion of the North Pacific sea-ice extent is unlikely to have contributed substantially to the EEP cooling. Unlike the Peru Current, the eastern boundary California current does not directly source the EEP, but feeds the North Equatorial Current (centered at approximately 20°N) [1].

The EEP temperature response to the sea-ice forcing occurs rapidly over model years 50 to 120. In contrast, the deep ocean response to sea-ice forcing is smaller and continuous throughout the 200 yrs of integration (Fig. 4). The decadal response time of the EEP, and its independence from deep ocean temperature, support our conclusion that high-latitude anomalies are propagating through the wind-driven thermocline circulation rather than the deep ocean circulation. This mechanism for transporting high-latitude climate signals to the tropics in FOAM was previously described and diagnosed in Lee and Poulsen [23], and is consistent with modern oceanographic processes in the Pacific Ocean [33,35]. In the modern ocean, EEP thermocline waters flow to the WEP through the equatorial currents [1]. As a consequence, the upwelling of cold mid-latitude waters into the EEP cools, to some degree, the entire tropical Pacific Ocean.

An analysis of the local energy budget provides further support that sea ice substantially impacts the ocean heat transport into the tropics. In the LGM-ICE experiment, the ocean heat flux to the EEP and WEP is reduced by 44% (39 W m^{-2}) and 29% (25 W m^{-2}). This reduction is a consequence of the advection of cooler waters through the tropical ocean. The reduced ocean heat flux is compensated by reductions in outgoing latent and longwave fluxes (Table 3), which are strongly linked to SST. The difference in the ocean heat flux between the EEP and WEP is likely due to mixing within the tropical ocean and local radiation, which effectively heats the tropical seawater along its path from east to west. In the modern tropical Pacific, clouds strongly influence the local radiation budget, generally decreasing the downward shortwave flux and increasing the downward longwave flux. Changes in tropical cloud amount and distribution between experiments could potentially provide an important feedback on the tropical SST gradient. However, an analysis of cloud

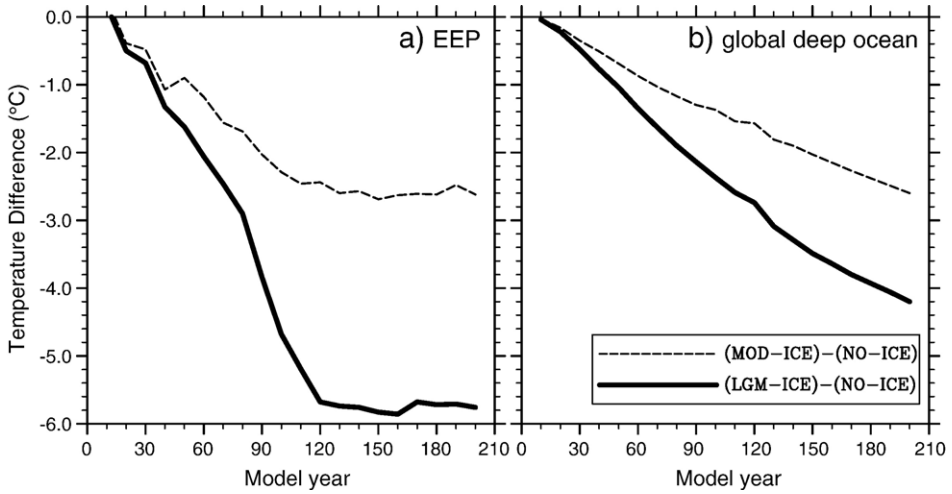

Fig. 4. Mean-annual seawater temperature differences (°C) in (a) the eastern equatorial Pacific upper ocean and (b) the global deep ocean through time (model years). The EEP upper ocean temperature differences were calculated between the sea surface and a depth of 150 m for the domain within 3.5°S–3.5°N and 92°E–103°E (Fig. 3a). The global deep ocean temperature differences were calculated between 200 and 5000 m.

Table 3
Net sea-surface energy fluxes

Term	LGM-ICE		NO-ICE		(LGM-ICE)–(NO-ICE)	
	WEP	EEP	WEP	EEP	WEP	EEP
Shortwave flux	620.5	604.6	644.5	638.0	−24.0	−33.4
Longwave flux	−426.5	−413.6	−456.3	−450.4	29.8	36.8
Sensible heat flux	−0.2	−2.2	−4.8	−4.3	4.6	2.1
Latent heat flux	−84.0	−61.2	−98.7	−94.7	14.7	33.5
Ocean heat flux	−109.8	−127.6	−84.7	−88.6	−25.1	−39.0

Energy fluxes are calculated for the eastern equatorial Pacific (EEP) (3.5°S–3.5°N, 92°E–103°E) and the western equatorial Pacific (WEP) (3.5°S–3.5°N, 150°W–164°W). The domain for the EEP and WEP area averages are illustrated in Fig. 3a (black boxes). Positive (negative) fluxes represent gain (loss) from the sea surface (in W m^{-2}). Sea surface energy fluxes are calculated for the LGM-ICE (left column) and NO-ICE experiments (center column), and the difference between the two experiments (left column).

forcing indicates that this is not the case; cloud forcing does not differ substantially between experiments.

As expected from the Bjerknes feedback [2], the increase in the east–west SST gradient intensifies the Walker circulation in the Pacific, as demonstrated by differences in the vertical pressure velocity and zonal winds between the LGM-ICE and MOD-ICE experiments (Fig. 5). In the LGM-ICE case, upward motion in the WEP increases by up to 15%, while subsidence in the EEP is up to 30% greater. In addition, the velocity of the Trade Winds and high-level Westerlies increase (Fig. 5), also implying an increase in the Walker Circulation. In contrast, the tropical meridional overturning circulation (Hadley circulation) weakens seasonally with the maximum overturning decreasing by as much as 10%. The Hadley cell response is consistent with analyses of modern observational data that report a weakened Hadley cell during times of enhanced zonal SST gradient and stronger Walker circulation (i.e. La Nina episodes) [36]. The positions of the Hadley cell and the Intertropical Convergence Zone show no significant change.

3.2. Atmospheric CO_2 forcing and tropical Pacific climate

In this section, we explore whether the evolution of the tropical Pacific could have happened in the absence of significant sea-ice forcing. Following the hypothesis of Medina-Elizalde and Lea [8] that the long-term depletion of atmospheric CO_2 controlled the tropical Pacific SSTs, we test the influence of CO_2-radiative forcing on the equatorial Pacific. Because the sea-ice model has been "turned off", differences in the NO-ICE and NO-ICE380 experiments exclude any sea-ice feedbacks to radiative forcing.

The reduction in atmospheric CO_2 from 380 to 200 ppm lowers tropical SSTs by ~0.8 °C zonally in FOAM but actually decreases the tropical Pacific SST gradient by ~0.4 °C (Fig. 6a). The tropical cooling is associated mainly with decreases in surface radiative heating and ocean heat flux (Table 3). However, in comparison to the sea-ice experiments (see Section 3.1), the decrease in ocean heat flux is very modest; the ocean heat flux is reduced by ~6% in both the EEP and WEP (Table 3). The reduced tropical SST gradient is primarily due to an increase in WEP low cloud coverage, which reduces the surface radiative heating in the WEP relative to the EEP. In sum, the model results indicate that pure radiative forcing, in the absence of sea-ice feedbacks, is not an effective mechanism for reducing the Pacific SST gradient.

3.3. Sea-ice and radiative forcing of tropical Pacific climate

In Sections 3.1 and 3.2, we found that sea ice and CO_2 have opposing influences on the tropical Pacific SST gradient: Southern Hemisphere sea ice enhances

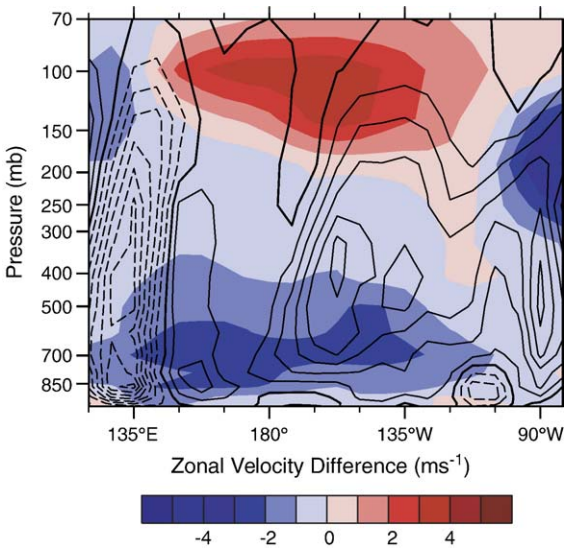

Fig. 5. Mean-annual vertical pressure velocity (Pa s^{-1}) (contours) and zonal velocity (m s^{-1}) (color contours) differences between the LGM-ICE and MOD-ICE experiments. Positive (negative) vertical velocity differences indicate enhanced subsidence (upward motion). Positive (negative) zonal velocity indicates increased eastward (westward) flow. Note from the vertical velocity differences that EEP subsidence and WEP upward motion is enhanced. Also, zonal velocity differences show an increase in the Trades and westward flow aloft.

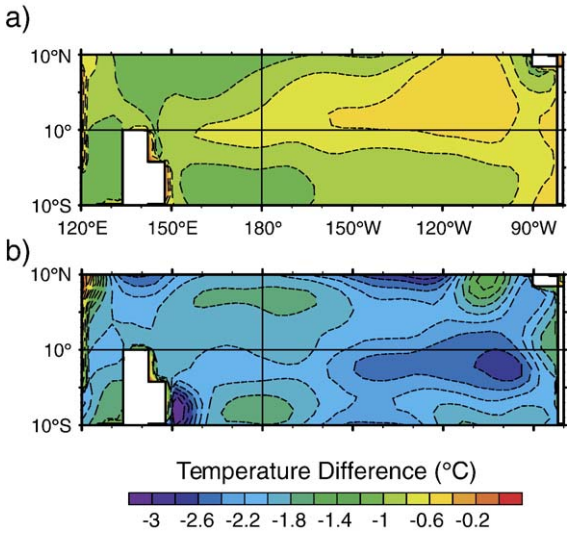

Fig. 6. Mean-annual SST differences (°C) in the equatorial Pacific Ocean between (a) the NO-ICE and NO-ICE380 experiments and, (b) the LGM-ICE and LGM-ICE380 experiments. Note that equatorial Pacific SST gradient is strengthened only with the presence of sea ice. The contour interval is 0.2 °C.

the gradient; reductions in CO_2-radiative forcing decrease the gradient. Because radiative forcing is likely to invoke a sea-ice feedback, we evaluate the effect of reducing CO_2 on the tropical Pacific climate with an active sea-ice margin by comparing LGM-ICE and LGM-ICE380 experiments. Reducing atmospheric CO_2 from 380 to 200 ppm resulted in a 24% increase in winter sea-ice area (Table 1). Tropical SSTs decreased by ~2.0 °C, and the east–west SST gradient increased by ~0.8 °C (Fig. 6b). This result is consistent with Knutson and Manabe [37], which demonstrated a reduction in tropical Pacific SST gradient with an increase in atmospheric CO_2 from 1xPAL (present day level) to 4xPAL. As in the previous experiments (Section 3.1), the intensification of the east–west SST gradient in FOAM results from upwelling of colder waters in the EEP and the associated decrease (~12%) in ocean heat flux. This result indicates that a secular decrease in atmospheric CO_2 could have driven the evolution of the tropical Pacific thermal gradient, but only in as much as CO_2 regulated Plio–Pleistocene sea ice.

4. Discussion

4.1. The tropical ocean–sea ice hypothesis

Proxy records of seawater temperature indicate that the equatorial Pacific surface temperature gradient increased by 2 °C from the Pliocene to the present day due to the cooling of the EEP [5–8]. Between the Pliocene and late Pleistocene glacial periods, the east–west SST gradient may have increased by more than 4 °C [6,7]. The sea-ice sensitivity experiments described here support the hypothesis that an increase in Southern Hemisphere, high-latitude sea ice could account for the Plio–Pleistocene intensification of the tropical Pacific thermal gradient. Moreover, the model-predicted increase in the east–west SST gradient is consistent with the proxy data; the Pliocene to glacial increase in sea ice, represented by the LGM-ICE and NO-ICE experiments, led to an increase of approximately 3.5 °C. We reiterate that this intensification of the tropical Pacific SST gradient is due solely to a change in sea-ice area; no other boundary conditions were modified. As a result, the model results should not be considered a prediction of past SST gradients, but rather a ball-park estimate of the potential influence of sea ice on tropical Pacific SST gradients. On the basis of the CO_2 sensitivity experiments (see Section 3.2), it is likely that an increase in sea ice in combination with a reduction in atmospheric CO_2 would result in a somewhat smaller increase in Pacific SST gradient.

Sea ice is an attractive mechanism for driving tropical climate change because paleoceanographic evidence indicates that the Southern Ocean sea-ice area increased substantially through the Plio–Pleistocene and between interglacial and glacial times [21,31,38–41]. Geological evidence of reduced sea-ice coverage in the Pliocene Southern Ocean includes low abundances of diatom assemblages that are typically associated with sea ice [21,42]; the deposition of marine deposits in regions presently covered by sea ice [43]; the presence of fossils of dolphins that lived in open-water environments [44]; and a sea-ice proxy based on the chain length of marine diatoms (the *Eucampia* index) [21]. In Prydz Bay, East Antarctica, the sea-ice coverage was only ~45% of its modern extent and may at time have been completely absent [21]. Although the position of the Pliocene sea-ice edge is not known with certainty, there is considerable evidence that it was less extensive than at any time since.

Likewise, glacial–interglacial changes in sea ice are also uncertain; however differences between last glacial and modern sea-ice extents suggest that sea ice was likely more extensive during glacial intervals. From the occurrences of ice-rafted debris, changes in foraminiferal and radiolarian faunal assemblages, and lithological boundaries between diatomaceous ooze and terrigenous silt, CLIMAP [39] estimated that the LGM Southern Hemisphere sea-ice margin extended to 45°S in the Atlantic and Indian Oceans and 55°S in the Pacific

Ocean. Gersonde et al. [41] used the abundance patterns of *Fragilariopsis curta* and *Fragilariopsis cylindrus* to calculate a 60–70% increase in Southern Ocean winter sea-ice coverage during the last glacial relative to the present. The cause of the increase in Southern Ocean sea ice through the Plio–Pleistocene and between interglacial–glacial cycles is not known with certainty but was likely related to reductions in atmospheric CO_2 and other GHGs (greenhouse gas) [34,45], orbital forcing, oceanic upwelling [46], deep-ocean cooling [47], and dynamics of the Antarctic ice sheet [48]. A particularly appealing notion is that the Western Antarctic Ice Sheet, because of its location and its dynamic history (e.g. [49,50]), may have had a substantial influence on sea ice in the southern South Pacific Ocean.

4.2. Study limitations

The purpose of this study is to evaluate the impact of sea ice on the equatorial Pacific rather than to simulate specific time slices. For this reason, identical model boundary conditions representing LGM conditions were used in each experiment; these boundary conditions are not, and were not intended to be, representative of Pliocene and interglacial times. The tropical Pacific SST gradient is likely to be sensitive to time-specific boundary conditions, particularly to the degree that they influence the proportion of sea ice (or the seawater temperature difference) between the high-latitude North and South Pacific. We also caution that our "tuning" of sea ice is not defensible from a physical standpoint. This device, which can be considered analogous to increasing freshwater fluxes in North Atlantic hosing experiments (e.g. [51–53]), was employed to obtain sea-ice margins that approximate those of glacial, interglacial, and Pliocene times. Like the North Atlantic hosing experiments, the sea-ice tuning is not strictly conservative; the artificial reduction in sea ice effectively removes latent energy of fusion (i.e. the energy that would have been used to freeze the sea ice) from the high latitudes. To further evaluate our hypothesis, climate simulations of these time slices with fully dynamic sea-ice models, and thus explicit sea-ice predictions, should be compared.

Because the purpose of this study was to examine the surface and thermocline circulations, the FOAM experiments were integrated for 200 yrs. Our analysis of global and eastern equatorial upper ocean (0–150 m) temperatures shows that temperature response to sea-ice forcing occurs in ~120 yrs (Fig. 4) by which point temperatures in these regions have stabilized. After 200 yrs, deep-ocean temperatures continue to change at rates of 0.006, −0.007 and −0.012 °C per decade in the NO-ICE, MOD-ICE and LGM-ICE experiments. The different tendencies in the shallow and deep oceans indicate that these regions are largely uncoupled; however, it is possible that further deepwater cooling could contribute to cooling of the eastern equatorial Pacific.

4.3. Summary and implications for Plio–Pleistocene climate evolution

That the tropical Pacific underwent a major reorganization in the Plio–Pleistocene is well documented [5–9]. Here, we present a specific mechanism, the cooling of the EEP through the upwelling of anomalously cold waters from the South Pacific, to explain the enhanced tropical Pacific SST gradient evidenced in marine proxy records. Our mechanism relies upon changes in Plio–Pleistocene sea ice that have been observed in the marine record (Section 4.1). The ultimate cause of Plio–Pleistocene sea-ice evolution is uncertain, but several possibilities exist including GHG variability. The sea-ice mechanism implies that the high-latitude Southern Hemisphere has been a climate puppeteer of sorts manipulating its tropical marionette, an idea that is consistent with observations that tropical SST coincided with Antarctic air temperature in the late Pleistocene [20].

On the basis of marine proxy data, it has been proposed that the strengthening of the SST gradient across the tropical Pacific and the intensification of the Walker circulation may have played a role in the onset and/or intensification of Northern Hemisphere glaciation, either as threshold events [7] or as a long-term conditioning [5]. Climate model results of the LGM support this idea; tropical SST patterns have been shown to have a substantial influence on glacial mass balance in the Northern Hemisphere [54]. Our model results are also generally consistent with this hypothesis; in the LGM-ICE experiment with cool tropical SSTs and an intensified SST gradient, mid- and high-latitude continental surface temperatures are several degrees cooler than in the NO-ICE case. In addition, continental snowfall is shifted southward toward the mid-latitudes. Though our experiments are highly idealized, we note that these tendencies would support the expansion of Northern Hemisphere glaciation. On the basis of these results, we speculate that conditioning for the intensification of Northern Hemisphere glaciation may have started with Southern Hemisphere cooling and sea-ice expansion. Southern Hemisphere cooling may have been transmitted through the thermocline circulation to the tropics, inducing cooling and intensification of the east–west SST gradient. Through atmospheric and

oceanic teleconnections, tropical climate changes may have then favored ice-sheet growth in the high latitudes of the Northern Hemisphere.

Acknowledgements

This research was supported by the National Science Foundation grant ATM-0432503 to C.J. Poulsen. We gratefully acknowledge M. Delaney, W. Ruddiman, and two reviewers for their constructive comments.

References

[1] G.L. Pickard, W.J. Emery, Descriptive Physical Oceanography, fifth ed. Butterworth Heinemann, Burlington, 1990.
[2] J. Bjerknes, Atmospheric teleconnections from the equatorial Pacific, Mon. Weather Rev. 97 (1969) 163–172.
[3] P. Molnar, M.A. Cane, El Niño's tropical climate and teleconnections as a blueprint for pre-Ice Age climates, Paleoceanography 17 (2002), doi:10.1029/2001PA000663.
[4] A.C. Ravelo, P.S. Dekens, M. McCarthy, Evidence for El Nino-like conditions during the Pliocene, GSA Today 16 (2006), doi:10.1130/1052-5173.
[5] A.C. Ravelo, D.H. Andreasen, M. Lyle, A.O. Lyle, M.W. Wara, Regional climate shifts caused by gradual global cooling in the Pliocene epoch, Nature 429 (2004) 263–267.
[6] T. de Garidel-Thoron, Y. Rosenthal, F. Bassinot, L. Beaufort, Stable sea surface temperatures in the western Pacific warm pool over the past 1.75 million years, Nature 433 (2005) 294–298.
[7] E.L. McClymont, A. Rosell-Melé, Links between the onset of modern Walker circulation and the mid-Pleistocene climate transition, Geology 33 (2005) 389–392.
[8] M. Medina-Elizalde, D.W. Lea, The Mid-Peistocene Transition in the Tropical Pacific, Science 310 (2005) 1009–1012.
[9] K.T. Lawrence, Z. Liu, T.D. Herbert, Evolution of the eastern tropical Pacific through Plio–Pleistocene glaciation, Science 312 (2006) 79–83.
[10] S.G. Philander, A.V. Federov, Role of tropics in changing the response to Milankovitch forcing some three million years ago, Paleoceanography 18 (1045) (2003), doi:10.1029/2002PA000837.
[11] G. Bocaletti, R.C. Pakanowski, S.G.H. Philander, A.V. Federov, The thermal structure of the upper ocean, J. Phys. Oceanogr. 34 (2004) 888–902.
[12] M. Sarnthein, K. Winn, J.-C. Duplessy, M.R. Fontugne, Global variations of surface ocean productivity in low and mid latitudes: influence on CO_2 reservoirs of the deep ocean and atmosphere during the last 21,000 years, Paleoceanography 3 (1988) 361–399.
[13] N.G. Pisias, D.K. Rea, Late Pleistocene paleoclimatology of the central equatorial Pacific: sea surface response to the southeast tradewinds, Paleoceanography 3 (1988) 21–37.
[14] D.K. Rea, The paleoclimate record provided by eolian deposition in the deep sea: the geologic history of wind, Rev. Geophys. 32 (1994) 159–195.
[15] D.J. Andreasen, A.C. Ravelo, Tropical Pacific ocean thermocline depth reconstructions for the Last Glacial Maximum, Paleoceanography 12 (1997) 395–413.
[16] L. Beaufort, T. de Garidel-Thoron, A.C. Mix, N.G. Pisias, ENSO-like forcing on oceanic primary production during the Late Pleistocene, Science 293 (2001) 2440–2444.
[17] A.B.G. Bush, S.G.H. Philander, The role of ocean–atmosphere interactions in tropical cooling during the Last Glacial Maximum, Science 279 (1998) 1341–1344.
[18] C.D. Hewitt, R.J. Stouffer, A.J. Broccoli, J.F.B. Mitchell, P.J. Valdes, The effect of ocean dynamics in a coupled GCM simulation of the Last Glacial Maximum, Clim. Dyn. 20 (2003) 203–218.
[19] A. Timmermann, F. Justino, F.-F. Jin, U. Krebs, H. Goosse, Surface temperature control in the North and tropical Pacific during the Last Glacial Maximum, Clim. Dyn. 23 (2004) 353–370.
[20] D.W. Lea, D.K. Pak, H.J. Spero, Climate impact of Late Quaternary equatorial Pacific sea surface temperature variations, Science 289 (2000) 1719–1724.
[21] J.M. Whitehead, S. Wotherspoon, S.M. Bohaty, Minimal Antarctic sea ice during the Pliocene, Geology 33 (2005) 137–140.
[22] CLIMAP Project members, The surface of the Ice-Age Earth, Science 191 (1976) 1131–1137.
[23] S.-Y. Lee, C.J. Poulsen, Tropical Pacific climate response to obliquity forcing in the Pleistocene, Paleoceanography 20 (2005) PA4010, doi:10.1029/2005PA001161.
[24] R.L. Jacob, Low frequency variability in a simulated atmosphere–ocean system, PhD thesis University of Wisconsin, (1997) 159 pp.
[25] J.T. Kiehl, J.J. Jack, G.B. Bonan, B.A. Boville, D.L. Williamson, P.J. Rasch, The national center for atmospheric research community climate model: CCM3, J. Climate 11 (1998) 1131–1149.
[26] L. Wu, Z. Liu, R.G. Gallimore, R. Jacob, D. Lee, Y. Zhong, A coupled modeling study of Pacific decadal variability: the Tropical mode and the North Pacific mode, J. Climate 15 (2003) 1101–1120.
[27] A.J. Semtner, A model for the thermodynamic growth of sea ice in numerical investigations of climate, J. Atmos. Sci. 6 (1976) 379–389.
[28] Z. Liu, S. Shin, P. Behling, W. Prell, M. Trend-Staid, S.P. Harrison, J.E. Kutzbach, Dynamical and observational constraints on tropical Pacific sea surface temperature at the Last Glacial Maximum, Geophys. Res. Lett. 27 (2000) 105–108.
[29] C.J. Poulsen, R.T. Pierrehumbert, R.L. Jacob, Impact of ocean dynamics on the simulation of the Neoproterozoic "snowball Earth", Geophys. Res. Lett. 28 (2001) 1575–1578.
[30] S.P. Harrison, J.E. Kutzbach, Z. Liu, P.J. Bartlein, B. Otto-Bliesner, D. Muhs, I.C. Prentice, R.S. Thompson, Mid-Holocene climate of the Americas: a dynamical response to changed seasonality, Clim. Dyn. 21 (2003) 663–688.
[31] X. Crosta, J.J. Pichon, Reappraisal of Antarctic seasonal sea-ice at the Last Glacial Maximum, Geophys. Res. Lett. 25 (1998) 2703–2706.
[32] P. Gloersen, W.J. Campell, D.J. Cavalierei, J.C. Comiso, C.L. Parkinson, H.J. Zwally, Arctic and Antarctic sea ice, 1978–1987: satellite passive-microwave observations and analysis: Washington D.C. NASA Spec. Publ. 511 (1992) 290.
[33] J.R. Toggweiler, K. Dixon, W.S. Broecker, The Peru upwelling and the ventilation of the South-Pacific thermocline, J. Geophys. Res., [Oceans] 96 (1991) 20467–20497.
[34] M.E. Raymo, B. Grant, M. Horowitz, G.H. Rau, Mid-Pliocene warmth: stronger greenhouse and stronger conveyor, Mar. Micropaleontol. 27 (1996) 313–326.
[35] S. Harper, Thermocline ventilation and pathways of tropical–subtropical water mass exchange, Tellus 52A (2000) 330–345.

[36] A.H. Oort, J.J. Yienger, Observed interannual variability in the Hadley circulation and its connection to ENSO, J. Climate 9 (1996) 2751–2767.
[37] T.R. Knutson, S. Manabe, Time-Mean Response over the Tropical Pacific to Increased CO_2 in a Coupled Ocean–Atmosphere Model, J. Climate 8 (1995) 2181–2199.
[38] J.D. Hays, J. Imbrie, N.J. Shackleton, Variation in the Earth's orbit: pacemaker of the ice ages, Science 194 (1976) 1121–1132.
[39] CLIMAP Project members, Seasonal reconstructions of the Earth's surface at the Last Glacial Maximum, Map Chart Ser. (Geol. Soc. Am) (1981) (MC-36).
[40] D.W. Cooke, J.D. Hays, Estimates of Antarctic ocean seasonal ice-cover during glacial intervals, Antarct. Geosci. 131 (1982) 1017–1025.
[41] R. Gersonde, A. Abelmann, U. Brathauer, S. Becquey, C. Bianchi, G. Cortese, H. Grobe, G. Kuhn, H.-S. Niebler, M. Segl, R. Sieger, U. Zielinski, D.K. Fütterer, Last glacial sea surface temperatures and sea-ice extent in the Southern Ocean (Atlantic–Indian sector): a multiproxy approach, Paleoceanography 18 (2003) 1061, doi:10.1029/2002PA000809.
[42] A.D. Mahood, J.A. Barron, Late Pliocene diatoms in a diatomite from Prydz Bay, East Antarctica, Micropaleontology 42 (1996) 285–302.
[43] J.M. Whitehead, B.C. McKelvey, The stratigraphy of the Pliocene–early Pleistocene Bardin Bluffs Formation, Amery Oasis, northern Prince Charles Mountains, Antarctica, Antarct. Sci. 13 (2001) 79–86.
[44] P.G. Quilty, Coastal East Antarctic Neogene sections and their contribution to the ice sheet evolution debate, Am. Geophys. Union Antarct. Res. Ser. 60 (1993) 251–264.
[45] J.R. Petit, J. Jouzel, D. Raynaud, N.I. Barkov, J.M. Barnola, I. Basile, M. Bender, J. Chappellaz, M. Davis, G. Delaygue, M. Delmotte, V.M. Kotlyakov, M. Legrand, V.Y. Lipenkov, C. Lorius, L. Pepin, C. Ritz, E. Saltzmen, M. Stievenard, Climate and atmospheric history of the past 420,000 from the Vostok ice core, Antarctica, Nature 399 (1999) 429–436.
[46] J.R. Marlow, C.B. Lange, G. Wefer, A. Rosell-Mele, Upwelling intensification as part of the Pliocene–Pleistocene climate transition, Science 290 (2000) 2288–2291.
[47] C.H. Lear, H. Elderfield, P.A. Wilson, Cenozoic deep-sea temperatures and global ice volumes from Mg/Ca in benthic foraminiferal calcite, Science 287 (2000) 269–272.
[48] P.J. Bart, J.B. Anderson, Relative temporal stability of the Antarctic ice sheets during the late Neogene based on the minimum frequency of outer shelf grounding events, Earth Planet. Sci. Lett. 182 (2000) 259–272.
[49] R.P. Scherer, A. Aldahan, S. Tulaczyk, G. Possnert, H. Engelhardt, B. Kamb, Pleistocene collapse of the West Antarctic Ice Sheet, Science 281 (1998) 82–85.
[50] H. Conway, B.L. Hall, G.H. Denton, A.M. Gades, E.D. Waddington, Past and future grounding-line retreat of the West Antarctic Ice Sheet, Science 286 (1999) 280–283.
[51] K. Dahl, A. Broccoli, R. Stouffer, Assessing the role of North Atlantic freshwater forcing in millennial scale climate variability: a tropical Atlantic perspective, Clim. Dyn. 24 (2005) 325–346.
[52] A.X. Hu, G.A. Meehl, Bering Strait throughflow and the thermohaline circulation, Geophys. Res. Lett. 32 (2005) L24610, doi:10.1029/2005GL024424.
[53] S. Rahmstorf, M. Cruicfix, A. Ganopolski, H. Goosse, I. Kamankovich, R. Knutti, G. Lohmann, R. Marsh, L.A. Mysak, Z. Wang, A.J. Weaver, Thermohaline circulation hysteresis, Geophys. Res. Lett. 32 (2005) L23605, doi:10.1029/2005GL023655.
[54] J.H. Yin, D.S. Battisti, The importance of tropical sea surface temperature patterns in simulations of Last Glacial Maximum climate, J. Climate 14 (2001) 565–581.
[55] A.L. Berger, Long term variations of daily insolation and Quaternary climatic changes, J. Atmos. Sci. 35 (1978) 2362–2367.
[56] W.R. Peltier, Ice age paleotopography, Science 265 (1994) 195–201.